NJC

Tunable emissions in lanthanide-based supramolecular metallogels

Journal:	*New Journal of Chemistry*
Manuscript ID	NJ-COM-10-2023-004692.R1
Article Type:	Communication
Date Submitted by the Author:	10-Nov-2023
Complete List of Authors:	Lee, Eun Gyu; Gyeongsang National University Han, Hyeon Min; Gyeongsang National University Jung, Jong Hwa; Gyeongsang National University, Chemistry Jung, Sung Ho; Gyeongsang National University

COMMUNICATION

Tunable emissions in lanthanide-based supramolecular metallogels

Eun Gyu Lee, [a] Hyeon min Han, [a] Jong Hwa Jung*[a] and Sung Ho Jung*[a]

Received 00th January 20xx,
Accepted 00th January 20xx

DOI: 10.1039/x0xx00000x

We have developed a tunable emissive supramolecular metallo-gel functionalized with lanthanide coordination bond using a low molecular weight gelator 1 having terminal terpyridine. In the presence of Tb(III) and Eu(III) ions, the coordination of lanthanides to a gelator 1 results in green and red emissive supramolecular metallogels, respectively. A supramolecular growth mechanism of 1-Tb that follows an isodesmic model has been observed, relying on delicate balances between non-covalent interactions. Furthermore, controlling the stoichiometry of lanthanide metal ions with respect to 1: Tb(III): Eu(III) leads to yellow and white light-emitting supramolecular bimetallic gels.

Supramolecular metallogels, in which complexes that contain metal ions self-assemble into nano/microstructures to immobilize solvents and utilize dynamic metal–ligand (M–L) coordination, have emerged as a powerful strategy for supramolecular systems.[1] These have potential for the development of functional soft materials, such as biomaterials, smart or adaptive materials, inkjet printing systems, color-tunable displays, chemical sensors, and electronic materials.[2-5] Including metal ions into supramolecular architectures requires the rational design of a monomer unit. The monomer requires a receptor unit to target metal ions, such as a ligand connected by a suitable alkyl chain with amide groups. Supramolecular metallogels can be formed through noncovalent interactions, such as coordination bonds, electrostatic effects, π-effects, van der Waals forces, and hydrophobic effects, which exhibit reversible, and stimuli-responsive characteristics [6,7] Through the design of the ligands, the choice of metal, and counter ions, as well as the self-assembly boundary conditions, including the metal ion-to-ligand ratio, concentration, solvent, ionic strength, and pH, are critical factors for achieving supramolecular metallogels.[8] In addition, metal ions provide various geometries and coordination numbers, which can introduce reactive, magnetic, optical, and electrochemical properties depending on the metal complexes.[9,10]

In this regard, through rational molecular design, and the utilization of dynamic coordination bonds, we can readily construct supramolecular metallogels with kinetic, thermodynamic, and functional properties.[11] This approach has recently been explored in supramolecular growth mechanisms, such as isodesmic, and cooperative models, which involve reversible supramolecular interactions.[12-14] Unique self-assembly processes lead to the formation of well-defined and highly organized structures, which allow for precise control over the emission properties of the resulting supramolecular gels.[15]

In addition, the 2,2′:6′,2″-terpyridine receptor is widely used as a ligand for metallo-supramolecular systems due to it being a strong π-acceptor toward and forming stable coordination complexes with a range of metal ions and its high thermal and oxidative stability.[16,17] Furthermore, terpyridine is complexed with lanthanide ions that could serve as antennas to enhance the luminescence intensity greatly. This well-established approach is commonly referred to as the antenna effect.[18,19] In particular, lanthanide-coordinated supramolecular gels have attracted increasing interest due to the unique features of Tb(III) and Eu(III) ions, such as high photochemical stability, narrow emission bands, and low toxicity.[20,21] Among the metal-coordinated materials, lanthanide M–L coordination supramolecular gels are being increasingly explored in the design of advanced functional materials because of their unique metal-controlled photoluminescence (4f–4f transitions).[22,23] In this context, lanthanide coordination-based supramolecular gels have a distinct advantage due to their reversible sol–gel behavior, which enhances their processability and facilitates the easy fabrication of large-area and flexible displays and portable sensing kits.[24]

[a] *Department of Chemistry and Research Institute of Natural Sciences, Gyeongsang National University, Jinju 52828, Republic of Korea*
Electronic Supplementary Information (ESI) available: [details of any supplementary information available should be included here]. See DOI: 10.1039/x0xx00000x

Recently, white light-emitting materials have been extensively studied because of their potential application in lighting and display devices.[25] These white light-emitting materials can be generated by adjusting the blue, green, and red light-emitting components, which often result from the coordination of lanthanide ions to suitable hosts or ligands.[26-29] For example, studies on lanthanide-based luminescent gels by Gunnlaugsson, Maji, and co-workers[30-32] discussed low molecular weight gelators that showed various material properties, including tunable luminescence, and white light emission. These strategies have been proposed to achieve white luminescence. However, the investigation of supramolecular bimetallic gels that undergo supramolecular assembly remains a significant challenge for various applications, particularly fine-tunable color emission.

In this study, we demonstrate the potential of supramolecular metallogels and their emission properties. The complexation of **1** via terpyridine with lanthanide metal ions, such as Tb(III) and Eu(III) ions, results in supramolecular metallogels that exhibit green and red emissions, respectively. Furthermore, through precise control of the stoichiometry in **1**, the Tb(III):Eu(III) ratio allows for yellow and white emissions. The deliberate design of metal-coordination bonds enables us to tailor the emission properties of supramolecular metallogels, which can eventually achieve white light-emitting supramolecular bimetallic gels.

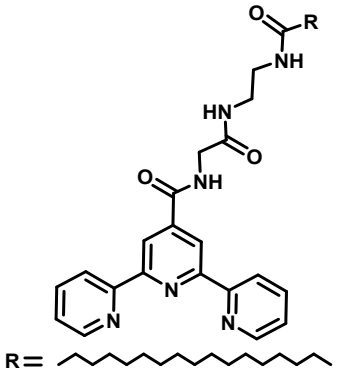

1

We synthesized ligand **1**, which incorporated a terpyridine moiety-tailored amide group with an alkyl chain, using a high-yield amidation reaction. The terpyridine moiety is well known for its excellent coordination abilities, particularly with lanthanide ions.[33] Ligand **1** was confirmed by ^{1}H, ^{13}C, and electrospray ionization mass spectrometry (ESI-MS) analyses (Supporting information S19-S27).

We performed a titration of **1** (1×10^{-6} M) with a methanolic solution of $Tb(NO_3)_3.6H_2O$ and $Eu(NO_3)_3.6H_2O$ (1×10^{-4} M). The corresponding ultraviolet–visible (UV-Vis) absorption and emission spectra were recorded (Fig. S1 and S2). Notably, enhanced emission in the Tb(III) titration suggested the formation of a complex between Tb(III) and **1**. In the presence of Tb(III) ions (1.0–9.0 equiv.), enhanced emission at 550 nm was observed, with identical behavior observed in the case of Eu(III). In addition, the association constant (K_a) of the Tb (III) and Eu(III) ions with **1** was calculated to be 1.5×10^3 and 1.7×10^3 M^{-1}, respectively, using the Benesi–Hildebrand plot (Fig. S3).

Next, we examined the gelation propensity of **1** for Tb (III) and Eu(III) in a mixture of MeOH and H_2O (v/v, 1/1). The lanthanide ions and **1** were taken in a molar ratio of 1:1 in the mixture of MeOH and H_2O (v/v, 1/1), respectively. After heating the reaction mixture to 60°C and then cooling it to room temperature, blue, green, and red emissive supramolecular metallogels for **1**, **1** with Tb(III) and Eu(III) were obtained, respectively (Fig. 1 and S4). In addition, the critical gelation concentration (CGC) of the **1, 1**-Tb, and **1**-Eu were estimated to be ~ 0.7 % (w/v) (Fig. S5)

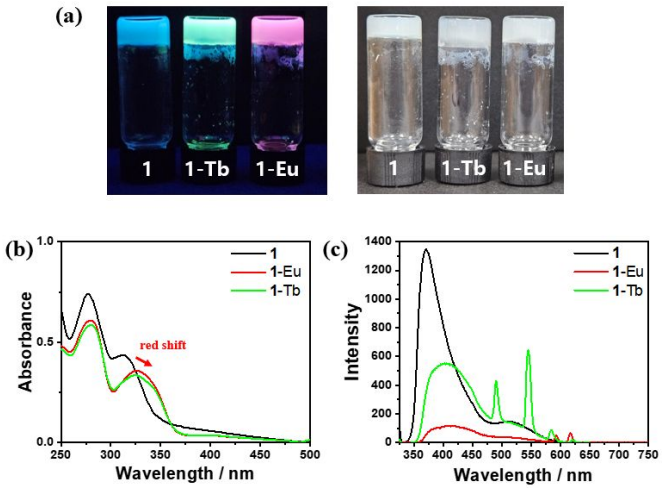

Fig. 1 (a) Photograph of supramolecular gels (1.0 wt%) of **1**(blue), **1**-Tb(green), and **1**-Eu(red) under UV light and ambient light. (b) UV-Vis absorption and (c) emission spectra of **1** (0.1 mM), **1**-Tb, and **1**-Eu in the mixture of MeOH and water (v/v, 1:1) (λ_{ex} = 322 nm).

The UV-Vis absorption band of the **1**-Tb gel was slightly red-shifted compared to that of the **1** gel (Fig. 1b). It exhibited an absorption band at 284 nm, which was attributed to $\pi \rightarrow \pi^*$ transitions of the terpyridine group. Notably, a broad shoulder band at 322 nm was also observed, suggesting the formation of Tb(III) and Eu(III) ions with a terpyridine group of **1** in a 1:1 stoichiometry, which was further confirmed by ESI-MS (Fig. S6 and S7).[34] The corresponding emission spectrum of **1**-Tb (λ_{ex} = 322 nm) showed a decrease in intensity at 370 nm. This quenching directly resulted from the complexation of Tb(III) ions to terpyridine moieties, accompanied by the appearance of sharp peaks at 490, 546, 587, and 623 nm. These peaks were attributed to the $^5D_4$–^7F_J (J = 6–3) transitions of Tb(III) (Fig. 1b). This complex formation resulted in an energy transfer from the terpyridine of **1** to Tb(III). Similar absorption and emission spectral changes were also observed when the above experiments were carried out using Eu(III) ion (Fig. S8). However, the emission spectrum exhibited weak bands at 592 and 618 nm, which was assigned to the $^5D_0$–$^7F_1$ and $^5D_0$–$^7F_2$ transition of Eu(III) ion, and a feeble decrease in emission at 370 nm (Fig. 1c). These results indicate a weak energy transfer from the terpyridine moiety to Eu(III) compared to Tb(III).

We monitored changes in the temperature-dependent absorption spectra of the aggregated **1**-Tb in a diluted solution at 0.1 mM. When the solution was heated, the UV-Vis absorbance change at 340 nm exhibited a sigmoidal transition as a function of temperature, indicating the growth of **1**-Tb supramolecular gel following an isodesmic mechanism (Fig. S9).

An enthalpy of −104.6 kJ mol^{-1} for **1**-Tb aggregation was estimated by a fitting analysis using an isodesmic model.[35]

Fig. 2 SEM images of (a) **1**-Tb and (b) **1**-Eu gels (1wt%).

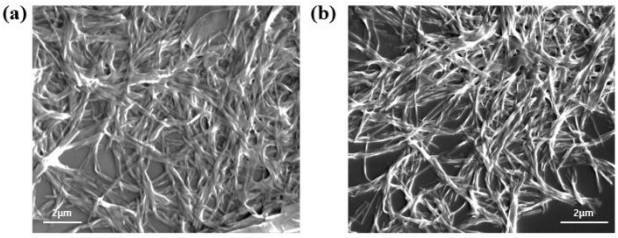

Field emission scanning electron microscopy (FE-SEM) images of the xerogel for **1**-Tb and **1**-Eu revealed a fibrous morphology. The nanofibers were several tens micrometers, with an approximate diameter of 80–120 nm (Fig. 2). The nanofibers of **1**-Tb and **1**-Eu were formed through gel formation by H-bonding between the amide groups and by π – π stacking between terpyridines. We carefully examined the hydrogen-bonding patterns of the **1**-Tb and **1**-Eu gels using Fourier-transform infrared (FTIR) spectroscopy. The N–H stretching frequencies of non-hydrogen-bonded N–H groups appeared around 3318 cm^{-1} in a sol state prepared in methanol, while those of intermolecularly hydrogen-bonded N–H amide groups shifted to lower energies of around 3290 cm^{-1} in a gel formation. In addition, intermolecularly hydrogen-bonded amide carbonyl groups (amide I band) C═O stretching appeared around 1640 cm^{-1}.[36,37] FTIR analysis revealed the presence of H-bonding in the gel formation, indicating intermolecular hydrogen-bonding interactions (Fig. S10). We also observed proton nuclear magnetic resonance (^{1}H NMR) spectral changes in the sol and gel states of **1**-Tb and **1**-Eu in MeOH-d_4 and in a mixture of D_2O and MeOH-d_4 (1:1 v/v) using NMR spectroscopy. The aromatic protons (H_3, H_4, and H_5) of the terpyridine moiety in **1** with $TbNO_3$ and $EuNO_3$ (1.0 equiv.) shifted to a lower field in a mixture of D_2O and MeOH-d_4 (1:1 v/v) (Fig. S11 and S12), indicating π–π stacking between the terpyridine moieties of **1**-Tb and **1**-Eu, respectively. The presence of H-bonding and π–π stacking in the gel formation was supported by NMR and FTIR analysis. To characterize the viscoelastic properties of the **1**, **1**-Tb, and **1**-Eu gels, strain and frequency sweeps rheology experiments were carried out at 25°C. These results revealed that the values of the storage modulus (G′) and loss modulus (G″) moved consistently within the linear viscoelastic region. Within this region, G′ exhibited a higher value over a relatively smaller strain range compared to G″, indicating stable viscoelasticity. In the frequency sweeps measurement, all the gels showed minimal frequency dependence of the storage modulus (G′) at a fixed small amplitude of strain (0.1 %). This phenomenon is a characteristic feature of metal-coordination gel materials (Fig. S13). Furthermore, when lanthanide ions were added, the G′ and G″ values of **1**-Tb and **1**-Eu gels increased by approximately 1.5- and 1.2-fold, respectively, compared to that of **1** gel. This indicates that the supramolecular metallogels formed with lanthanide ions were much stronger than the **1** gel formed without metal ions. Therefore, the higher G′ and G″ values of **1**-Tb and **1**-Eu gels compared to **1** gel could be attributed to intermolecular hydrogen-bond interactions and coordination bonds in the supramolecular network structure.

We investigated the modulation of supramolecular metallogel emissions by tuning the stoichiometry of the two lanthanides of **1**-Tb and **1**-Eu (green and red, respectively). **1**-Tb and **1**-Eu formed a homogeneous mixed gel in a mixture of MeOH and H_2O (v/v, 1/1) and exhibited yellow (Eu:Tb = 6:4) and white (Eu:Tb = 12:13) emissions at different ratios of Tb:Eu, under UV irradiation, respectively (Fig. 3). In addition, an FE-SEM image of the dry gel revealed entangled fibers with diameters ranging from 60 to 180 nm (Fig. S14). The presence of coordinated Tb(III) and Eu(III) in the xerogels for **1**- Tb, **1**-Eu, and a mixture of **1**- Tb and **1**-Eu (resulting in yellow and white emissive gels) was confirmed through energy dispersive X-ray spectroscopy (EDXS) analysis (Fig. S15-S18). Emission spectroscopy studies determined that the intensity of the **1**-Tb green band at 546 nm gradually increased and was accompanied by the **1**-Eu red band at 618 nm as a function of the Tb:Eu molar ratio, under excitation at 322 nm (Fig. 3c). By introducing a red emissive **1**-Eu into a green emissive **1**-Tb, the emission color of supramolecular metallogels can be precisely adjusted using an RGB approach. Consequently, the emission characteristics of supramolecular metallogels can be further finely tuned towards the production of yellow and white light. The color changes based on the emission spectra of a mixture

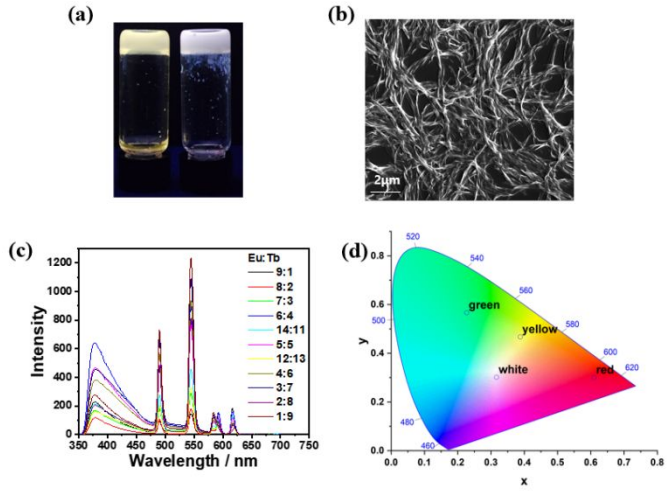

of **1**-Tb and **1**-Eu with different ratios of Tb and Eu in a gel formation were marked using a CIE program. Interestingly, the white light-emitting metallo-supramolecular gel showed strong signals at both 584 nm and 593 nm, assigned to the emission of **1**-Tb and **1**-Eu, respectively, merged to exhibit strong white light (Fig. 3). The CIE color coordinates of the white emissive gel were x = 0.316 and y = 0.302 in the white region.

Fig. 3 (a) Photograph of yellow (Eu:Tb = 6:4) and white (Eu:Tb = 12:13) emissive gels (1wt%) under UV light, respectively. (b) SEM image of the white gel. (c) Emission spectra of metallogels as a function of the Eu:Tb molar ratio (1wt%) and (d) CIE color coordinates of emissive supramolecular metallogels (λ_{ex} = 322 nm).

Conclusions

We demonstrated that terpyridine derivative, as ligands, form emissive supramolecular metallogels with Tb(III) and Eu(III) ions

in a mixture of MeOH and H_2O (v/v, 1/1) due to energy transfer from the terpyridine moiety to lanthanide ions. Furthermore, the aggregation of **1**-Tb, and **1**-Eu showed well-defined nanofiber structures that followed an isodesmic growth self-assembly process. Interestingly, fine-tuning of the emission properties of the supramolecular metallogels was achieved by precisely controlling the molar ratio of **1**:Tb:Eu during the formation of a homogeneously mixed gel, leading to yellow, and white emissive supramolecular bimetallic gels. We anticipate that the insights gained from this research will enhance the comprehension of emissive supramolecular metallogels and provide a solid foundation for designing and developing novel white emissive soft materials.

Conflicts of interest

There are no conflicts to declare.

Acknowledgements

This research was supported by the National Foundation of Korea (NRF) grant funded by the Korea government (MSIT) (RS-2023-00241926 and 2022R1A4A1022252).

References

1. S. A. Lim, S, H, Jung and J. H. Jung, *Bull. Korean Chem. Soc*. 2023, **44**, 322-331.
2. J. Li, L. Geng, G. Wang, H. Chu and H. Wei, *Chem. Mater.*, 2017, **29**, 8932-8952.
3. C. Kim, K. Y. Kim, J. H. Lee, J. Ahn, K. Sakurai, S. S. Lee and J. H. Jung, *ACS Appl. Mater. Interfaces*, 2017, **9**, 3799-3807.
4. A. Y. Tam and V. W. Yam, *Chem. Soc. Rev.*, 2013, **42**, 1540-1567.
5. C. D. Jones and J. W. Steed, *Chem. Soc. Rev.*, 2016, **45**, 6546-6596.
6. G. Z. Zhao, L. J. Chen, W. Wang, J. Zhang, G. Yang, D. X. Wang, Y. Yu and H. B. Yang, *Chem.*, 2013, **19**, 10094-10100.
7. Z. Liu, X. Zhao, Q. Chu and Y. Feng, *Molecules*, 2023, **28**.
8. Z. Liu, W. He and Z. Guo, *Chem. Soc. Rev.*, 2013, **42**, 1568-1600.
9. M. Cirulli, A. Kaur, J. E. M. Lewis, Z. Zhang, J. A. Kitchen, S. M. Goldup and M. M. Roessler, . *Am. Chem. Soc.*, 2019, **141**, 879-889.
10. F. S. Han, M. Higuchi and D. G. Kurth, . *Am. Chem. Soc.*, 2008, **130**, 2073-2081.
11. M. H. Chan and V. W. Yam, . *Am. Chem. Soc.*, 2022, **144**, 22805-22825.
12. M. M. Smulders, M. M. Nieuwenhuizen, T. F. de Greef, P. van der Schoot, A. P. Schenning and E. W. Meijer, *Chem.*, 2010, **16**, 362-367.
13. M. J. Mayoral, C. Rest, V. Stepanenko, J. Schellheimer, R. Q. Albuquerque and G. Fernandez, . *Am. Chem. Soc.*, 2013, **135**, 2148-2151.
14. P. A. Korevaar, S. J. George, A. J. Markvoort, M. M. Smulders, P. A. Hilbers, A. P. Schenning, T. F. De Greef and E. W. Meijer, *Nature.*, 2012, **481**, 492-496.
15. S. Panja and D. J. Adams, *Chem. Soc. Rev.*, 2021, **50**, 5165-5200.
16. C. Wei, Y. He, X. Shi and Z. Song, *Coord. Chem. Rev.*, 2019, **385**, 1-19.
17. S. S. M. Fernandes, M. Belsley, C. Ciarrocchi, M. Licchelli and M. M. M. Raposo, *Dyes Pigm.*, 2018, **150**, 49-58.
18. H. Q. Yin, X. Y. Wang and X. B. Yin, *J. Am. Chem. Soc.*, 2019, **141**, 15166-15173.
19. Y. W. Yip, H. Wen, W. T. Wong, P. A. Tanner and K. L. Wong, *Inorg. Chem.*, 2012, **51**, 7013-7015.
20. X. Z. Li, C. B. Tian and Q. F. Sun, *Chem. Rev.*, 2022, **122**, 6374-6458.
21. B. C. Roy and T. S. Mahapatra, *Soft Matter*, 2023, **19**, 1854-1872.
22. P. Zhang, N. Song, S. Liu, Q. Li, Y. Wang and B. Zhou, *J. Mater. Chem. C*, 2021, **9**, 6208-6216.
23. I. N. Hegarty, S. J. Bradberry, J. I. Lovitt, J. M. Delente, N. Willis-Fox, R. Daly and T. Gunnlaugsson, *Mater. Chem. Front.*, 2023, **7**, 906-916.
24. N. Alam, S. Mondal, S. K. S. Hossain, S. Sahoo and D. Sarma, *ACS Appl. Energy Mater.*, 2023, **1**, 1201-1212.
25. G. M. Farinola and R. Ragni, *Chem. Soc. Rev.*, 2011, **40**, 3467-3482.
26. O. Kotova, S. Comby, C. Lincheneau and T. Gunnlaugsson, *Chem. Sci.*, 2017, **8**, 3419-3426.
27. A. Ghazy, M. Lastusaari and M. Karppinen, *J.Mater.Chem.C*, 2023, **11**, 5331-5336.
28. N. A. Vazquez-Mera, J. R. Otaegui, R. S. Sanchez, G. Prats, G. Guirado, D. Ruiz-Molina, C. Roscini and J. Hernando, *ACS Appl. Mater. Interfaces*, 2019, **11**, 17751-17758.
29. M. Zhang, J. Xue, Y. Zhu, C. Yao and D. Yang, *ACS Appl. Mater. Interfaces*, 2020, **12**, 22191-22199.
30. P. Sutar, V. M. Suresh and T. K. Maji, *Chem. Commun.*, 2015, **51**, 9876-9879.
31. P. Verma, A. Singh and T. K. Maji, *Chem. Sci.*, 2020, **12**, 2674-2682.
32. M. Martinez-Calvo, O. Kotova, M. E. Mobius, A. P. Bell, T. McCabe, J. J. Boland and T. Gunnlaugsson, *J. Am. Chem. Soc.*, 2015, **137**, 1983-1992.
33. S. Y. Wang, J. H. Fu, Y. P. Liang, Y. J. He, Y. S. Chen and Y. T. Chan, *J. Am. Chem. Soc.*, 2016, **138**, 3651-3654.
34. O. Kotova, R. Daly, C. M. dos Santos, M. Boese, P. E. Kruger, J. J. Boland and T. Gunnlaugsson, *Angew. Chem.*, 2012, **51**, 7208-7212.
35. M. M. Smulders, M. M. Nieuwenhuizen, T. F. de Greef, P. van der Schoot, A. P. Schenning and E. W. Meijer, *Chem.*, 2010, **16**, 362-367.
36. T. A. Okamura, Nakagawa, J., *Inorg. Chem.*, 2013, **52**, 10812-10824.
37. M. Wehner, M. I. S. Rohr, M. Buhler, V. Stepanenko, W.Wagner and F. Wurthner, *J. Am. Chem. Soc.*, 2019, **141**, 6092-6107.

